

A study of Hilda asteroids

II. Compositional implications from optical spectroscopy*

M. Dahlgren¹, C.-I. Lagerkvist^{1,4}, A. Fitzsimmons², I.P. Williams³, and M. Gordon³

¹ Astronomical observatory, Box 515, S-75120 Uppsala, Sweden (Mats.Dahlgren@astro.uu.se, Claes-Ingvar.Lagerkvist@astro.uu.se)

² APS Division, Department of Pure and Applied Physics, The Queen's University of Belfast, Belfast BT7 1NN, Northern Ireland (A.Fitzsimmons@Queens-Belfast.ac.uk)

³ Astronomy Unit, School of Mathematical Sciences, Queen Mary and Westfield College, Mile End Road, London E1 4NS, UK (I.P.Williams@qmw.ac.uk, M.K.Gordon@qmw.ac.uk)

⁴ DLR, German Aerospace Research Establishment, Rudower Chausse 5, D-12489 Berlin, Germany

Received 9 April 1996 / Accepted 16 January 1997

Abstract. We obtained 49 reflectance spectra of 23 Hilda asteroids in the wavelength ranges 3850–7650 and 3850–10150 Å during two observing runs in 1992. The primitive D-types dominate and comprise 34 % of the numbered Hilda asteroids, while 28 % and 2 % are P and C-types, respectively. This is in contrast to the results of earlier investigations by Tedesco & Gradie (1982) and Gradie et al. (1989) who found fewer D-type asteroids in the Hilda group. We confirm the result by Dahlgren & Lagerkvist (1995) that there is a spectral slope - asteroid size relation among the Hilda asteroids, implying a size dependent surface composition. No evidence of absorption features are seen in the spectra of the P and D-types, in particular no features due to phyllosilicates are found, implying that no aqueous alteration of the surfaces has occurred. The absence of C-types within the Hilda group suggests that the C population is confined to smaller heliocentric distances than thought before, with very few C asteroids further out than the Cybele group. The phase reddening effect is absent for the P and D-types observed. Though it is not a Hilda member one spectrum of 279 Thule was obtained and is also presented.

Key words: asteroids

1. Introduction

Due to their likely pristine nature the asteroids in the outer edge of the asteroid belt may hold a number of clues to the origin and evolution of the asteroid belt and to the formation of the planetary system. The asteroids in the outer belt, which are

usually defined as objects with a semi-major axis > 3.3 AU, fall into three main groups. The Cybeles between 3.3-3.5 AU, the Hildas in the 3:2 resonance with Jupiter at 4.0 AU and the Trojans around the Lagrangian L4 and L5 points of Jupiter at 5.2 AU. These groups are populated by asteroids which are at one end of a compositional trend seen across the asteroid belt, with only low albedo C, P and D-type asteroids in the Hilda and Trojan regions (Tedesco & Gradie 1982, Gradie et al. 1989). Due to their large heliocentric distances, the outer belt asteroids have experienced less heating and are of a more pristine composition. They may also contain a large fraction of ice in their interiors (Bell et al. 1989).

Gradie & Veverka (1980) matched the spectral response of D-type asteroids using mixtures of organic material and hydrated silicates. However, later investigations by Jones et al. (1990) indicated that P and D-types appear to be anhydrous and Luu et al. (1994) did not find any IR absorption bands, indicative of organics, in the P and D-type asteroids they observed. At present the general out-line for the composition of the P and D-types is a mixture of organics, anhydrous silicates, opaque material and ice (Bell et al. 1989; Gaffey et al. 1989; Vilas et al. 1994). Pin-pointing the composition of P and D-types is especially difficult since no analogous meteorites have been found on Earth. Some indications of phyllosilicates on a few P-type asteroids have been reported by Vilas & Gaffey (1989). The first attempt to study outer belt asteroids by CCD spectroscopy was made by Vilas & Smith (1985). Further investigations have been carried out by Jewitt & Luu (1990), Vilas & McFadden (1992), Vilas et al. (1993a,b), Fitzsimmons et al. (1994), Dahlgren & Lagerkvist (1995) and Lazzarin et al. (1996). The variation of colours with heliocentric distance for D-type asteroids were studied by Lagerkvist et al. (1993), while Fitzsimmons et al. (1994) also addressed the question of a possible similarity to cometary nuclei.

Send offprint requests to: M. Dahlgren

* Partly based on observations collected at the European Southern Observatory, La Silla (Chile).

Focusing on the Hilda asteroids, Dahlgren & Lagerkvist (1995) (hereafter Paper I), increased the sample both in number and in size range, since existing data was heavily biased towards the few large Hilda asteroids. The smaller ($D \sim 50$ km) Hilda asteroids observed in Paper I were all D-type, indicating a taxonomic type – size relation among the Hilda asteroids.

This work presented here continues that described in Paper I, presenting results obtained from an additional 49 low resolution spectra in the optical wavelength region of 23 Hilda asteroids.

2. Observations

2.1. New Technology Telescope

Approximately half of the spectra were obtained during the nights of 1992 September 1 and September 2 with the 3.5m New Technology Telescope (NTT) at The European Southern Observatory, La Silla, Chile. The weather was photometric on both nights. The multi-mode instrument EMMI was used in the red spectroscopic medium dispersion mode giving a dispersion of 4.37 \AA per pixel. The detector used was a Thomson 1024 \times 1024 pixel CCD. The tracking of the telescope was adjusted to match the apparent motion of the targets. Wavelength calibration was performed with a Helium-Argon lamp. The wavelength range of the spectra are 3850 to 8270 \AA , however, due to possible second order overlap, only the wavelength range from 3850 to 7650 \AA was used. Exposure times were selected to give approximately the same signal-to-noise ratio (S/N) for all spectra of the asteroids. The peak S/N for most objects are between 55–70. Bias and flat-field frames were obtained on both nights. The solar analogue star HD 44594 (Cayrel de Strobel, 1990) was used but unfortunately it could only be observed at rather high airmass. No other good solar analogue star was observable near the meridian.

2.2. William Herschel Telescope

The spectra from 1992 October 31 and November 1 were obtained with the 4.2m William Herschel Telescope (WHT) at The Observatorio del Roque de los Muchachos on La Palma, Canary Islands, Spain. The ISIS double beam spectrograph with low dispersion gratings R158B and R158R was used. A spectral coverage from 3850 to 10150 \AA was obtained, with a dichroic giving a cross-over at $\sim 7100 \text{ \AA}$. Both the blue and red arms used an EEV P88300 CCD with 1242 \times 1152 pixels. An exposure time of 30 minutes was used for all but the brightest targets, where an exposure time of 20 minutes was used. The tracking was adjusted to follow the apparent motion of the targets. The dispersion of the spectra are 2.70 \AA per pixel in the blue and 2.72 \AA per pixel in the red. The wavelength calibration was made with a Copper-Argon lamp, exposed immediately after each spectrum to compensate for the small flexure of ISIS. Two solar analogue stars, HD 186427 and HD 28099 (Cayrel de Strobel, 1990), were observed at different airmasses. Bias and flat-fields were obtained on both nights. The observational circumstances for both observing runs are listed in Table 1.

3. Data reduction

All the acquired data was reduced using the ESO-Midas package. The bias and flat-field frames displayed no variation between the two nights at each telescope, thus, median bias and flat-field frames were constructed for each observing run. The general out-line of the method of spectroscopic data reduction can be found in Paper I and Fitzsimmons et al. (1994).

3.1. William Herschel Telescope

Since ISIS projects the incoming light on ~ 2400 pixels, the pixels in all frames were first binned two by two to increase the S/N. Due to a slight change in the wavelength range of the spectrograph after the flat-fields were taken, the large-scale intensity pattern was not the same on the flat-fields as on the target frames. This was solved by construction of normalized flat-fields to remove the pixel-to-pixel variations. The large-scale structure was later removed in the sky subtraction. The error introduced by the wavelength dependence of the pixel-to-pixel variations due to different wavelengths hitting the same pixel could not be corrected. The wavelength shift was 80 \AA and introduces $\sim 20 \%$ increased noise-level in the spectra.

After bias and flat-field corrections, the cosmic-hits were removed by interpolation of near-by pixels. The sky background was removed by fitting a polynomial to each column on each side of the spectra. Extraction of the spectrum was made by averaging the rows containing the spectrum. The rows were selected by examination of the profile perpendicular to the dispersion at different wavelengths. Then the wavelength calibration was performed. Due to the binning the final dispersion is $5.41 \text{ \AA}/\text{pixel}$ in the blue and $5.45 \text{ \AA}/\text{pixel}$ in the red part of the spectra. The error of the wavelength calibrations were 0.7 \AA and 0.1 \AA , respectively. The wavelength calibrated spectra were corrected for extinction with the standard extinction law at La Palma (King, 1985).

The solar analogue stars were treated in the same way as the asteroids. The extinction correction was checked by comparing the solar analogue spectra taken at different airmass. The differences were found to be small (Fig. 1), and the final solar analogue spectra is the mean of all solar analogue spectra observed on each night.

The asteroid spectra was divided by the mean solar analogue spectrum of the night to get the final spectra, and then the blue and red parts were combined into one spectrum. To remove the large spikes from cosmic-hits on the actual asteroid spectrum a median filter was applied which replaces pixels deviating by more than 30% from the median of the neighboring pixels, thereby, only removing the large spikes.

3.2. New Technology Telescope

The data from the NTT was reduced in the same way as the WHT data. In this case the error of the wavelength calibration was 0.8 \AA . The solar analogue star HD 44594 could only be observed at airmass in excess of 1.50 and so it was difficult carry out the extinction corrections for the HD 44594 spectra

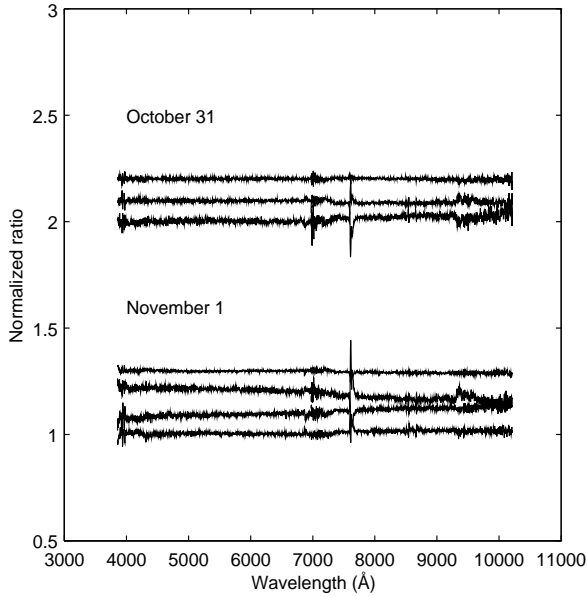


Fig. 1. Normalized residual solar analogue spectra. On October 31 the used solar analogue spectrum was constructed from three spectra taken at different airmass, while on November 1 four spectra were used. Each 'spectrum' in the figure is the residual from each spectrum compared to the used mean solar analogue spectrum. In the ideal case all of the spectra should be perfect lines. The two middle 'spectra' of November 1 show some small divergence from the ideal case. The uncertainty in the spectral slope parameter S' introduced into the asteroid spectra are below $0.1 \text{ \%}/10^3 \text{ \AA}$ on the first night and below $0.8 \text{ \%}/10^3 \text{ \AA}$ on the second night. The spectra are shifted vertically for clarity.

with the required accuracy using the mean extinction law of La Silla (Tüg, 1977). Indeed, doing this gave unrealistic slopes of the asteroid spectra and so HD 44594 could not be used. Since most of the asteroids were observed at low airmass we used the mean extinction of La Silla and the solar analogue stars HD 186427 and HD 28099 observed with the WHT.

For asteroids observed from both La Silla and La Palma, by dividing the extinction corrected spectra of the same asteroid taken with the two telescopes, it is easy to construct a differential response curve (DRC) describing the relative difference in instrument through-put, that is

$$DRC(\lambda) = \frac{F_{NTT}(\lambda)}{F_{WHT}(\lambda)} \quad (1)$$

where $F_{WHT}(\lambda)$ and $F_{NTT}(\lambda)$ is the flux at wavelength λ . The DRC was also smoothed to remove noise. An asteroid spectra from the NTT, divided with a solar analogue star ($\odot(\lambda)$) can then be found from

$$F_{NTT/\odot}(\lambda) = \frac{F_{NTT}(\lambda)}{DRC(\lambda)F_{\odot WHT}(\lambda)} \quad (2)$$

where $F_{\odot WHT}(\lambda)$ is the flux at wavelength λ from the solar analogue star observed with the WHT.

This procedure depends critically on the assumption that the reflected light from the asteroid is identical at both occasions.

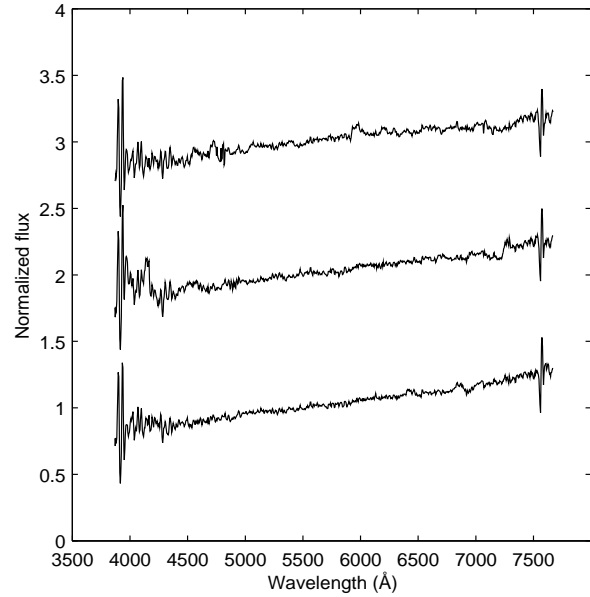


Fig. 2. The spectra of 1269 Rollandia ($F_{NTT/\odot}(\lambda)$) obtained using a response function from the three asteroids observed with both the NTT and the WHT.

There are two primary reasons why this assumption may not be true; (i) there can be changes in the albedo on the surface of the asteroid, (ii) the geometry was different during the two observing runs, leading to a colour change due to the different phase angles.

The best candidate to make the DRC from was 153 Hilda because of the high S/N of its spectra, and the number of spectra obtained during the NTT run. The relative rotational phase of Hilda during the three observations were 0.0, 0.5 and 0.7, using the rotation period of 153 Hilda, determined to 5.11 hours by Lagerkvist et al. (1996). Intercomparing the three spectra, they showed no significant variation. This rules out any large effects arising from albedo variations.

The change in observational geometry between the two data sets was small, giving a change in solar phase angle (α) of only $\sim 9^\circ$. The phase reddening effect, i.e. the reddening of asteroidal colours with increasing phase angle, is unknown for P and D-type asteroids, but the correction is probably minor for the phase angles in question here. This will be further discussed in Sect. 4.3.

To further check the DRC obtained by using the three spectra of 153 Hilda, we also used spectra from 1212 Francette and 1345 Potomac to construct other DRC's. These showed no significant variations from each other. In Fig. 2 the reflectance spectra of 1269 Rollandia are shown using the DRC from 153 Hilda, 1212 Francette and 1345 Potomac. From the outcome of these checks we feel confident that the DRC constructed from the spectra of 153 Hilda can be used to obtain reliable results out from the NTT data.

Table 1. The observational circumstance of all the Hilda asteroids. The ephemerides V -magnitude, heliocentric distance r , geocentric distance Δ and solar phase angle α are given for the hour closest to the middle of the exposure. The airmass is given for the middle of the exposure.

Hilda asteroid	mag V	r AU	Δ AU	α deg	airmass	date	telescope
153 Hilda	12.9	3.60	2.64	6.1	1.11	1/9 1992	NTT
	12.9	3.60	2.65	6.3	1.11	2/9 1992	NTT
	12.9	3.60	2.65	6.3	1.19	2/9 1992	NTT
334 Chicago	13.8	3.67	3.37	15.5	1.24	1/11 1992	WHT
	13.2	3.86	2.87	3.7	1.17	1/9 1992	NTT
	13.1	3.86	2.87	3.4	1.09	2/9 1992	NTT
361 Bononia	13.8	3.88	3.19	11.7	1.28	31/10 1992	WHT
	13.1	3.39	2.42	4.2	1.04	1/11 1992	WHT
	958 Asplinda	15.5	3.28	2.32	5.1	1.06	31/10 1992
1212 Francette	15.8	4.61	3.60	1.3	1.27	1/9 1992	NTT
	15.8	4.61	3.60	1.1	1.08	2/9 1992	NTT
	16.5	4.56	3.99	10.9	1.59	31/10 1992	WHT
1269 Rollandia	16.5	4.56	4.00	11.0	1.31	1/11 1992	WHT
	14.7	4.29	3.28	0.8	1.09	1/9 1992	NTT
	14.6	4.29	3.28	0.6	1.08	2/9 1992	NTT
1345 Potomac	15.5	4.28	3.74	11.9	1.31	1/11 1992	WHT
	15.8	4.20	3.25	5.3	1.09	1/9 1992	NTT
	15.8	4.20	3.24	5.1	1.07	2/9 1992	NTT
1439 Vogtia	16.1	4.11	3.38	10.3	1.36	1/11 1992	WHT
	16.7	4.35	3.41	5.2	1.16	2/9 1992	NTT
	16.9	4.32	3.55	9.2	1.20	1/11 1992	WHT
1529 Oterma	15.9	3.24	2.90	17.8	1.34	1/9 1992	NTT
	15.9	3.24	2.89	17.8	1.37	2/9 1992	NTT
	15.0	3.25	3.11	6.5	1.12	31/10 1992	WHT
1754 Cunningham	15.0	3.25	2.31	6.2	1.10	1/11 1992	WHT
	15.5	3.31	2.74	15.9	1.05	1/9 1992	NTT
	15.5	3.31	2.75	16.0	1.05	2/9 1992	NTT
2246 Bowell	16.8	4.32	3.37	4.9	1.13	1/9 1992	NTT
	16.8	4.33	3.38	4.6	1.15	2/9 1992	NTT
	17.2	4.33	3.58	9.4	1.30	31/10 1992	WHT
2483 Guinevere	16.4	3.43	2.70	12.7	1.18	31/10 1992	WHT
2959 Scholl	16.2	2.94	2.25	16.1	1.02	31/10 1992	WHT
3134 Kostinsky	15.5	3.09	2.20	9.9	1.04	31/10 1992	WHT
3202 Graff	16.4	4.28	3.29	3.6	1.15	1/9 1992	NTT
	16.4	4.28	3.30	3.8	1.14	2/9 1992	NTT
3415 Danby	16.0	3.22	2.61	15.5	1.02	31/10 1992	WHT
	16.0	3.22	2.60	15.3	1.01	1/11 1992	WHT
3557 Sokolsky	16.4	3.33	2.76	15.7	1.03	2/9 1992	NTT
3571 Milanstefanik	16.5	3.60	2.66	6.7	1.09	1/9 1992	NTT
	16.5	3.60	2.67	7.0	1.09	2/9 1992	NTT
3577 Putilin	16.8	4.31	3.31	1.8	1.09	1/9 1992	NTT
	16.8	4.31	3.31	2.1	1.08	2/9 1992	NTT
3694 Sharon	15.0	3.18	2.19	2.2	1.08	31/10 1992	WHT
3843 OISCA	16.3	3.60	2.82	11.4	1.27	2/9 1992	NTT
	15.9	3.56	2.62	5.8	1.17	31/10 1992	WHT
	15.9	3.56	2.62	6.1	1.28	1/11 1992	WHT
3923 Radzievskij	16.1	3.28	2.30	4.3	1.22	31/10 1992	WHT
	16.1	3.27	2.31	4.7	1.09	1/11 1992	WHT
4446 Carolyn	15.9	2.85	2.15	16.8	1.07	2/9 1992	NTT
279 Thule	15.4	4.31	3.78	12.2	1.01	2/9 1992	NTT

Table 2. Summary of the obtained spectral slopes S' and other relevant parameters.

Hilda asteroid	NTT		WHT		adopted mean S'	taxonomy		D km	albedo %	H mag
	spectral slope S'					this paper	Tholen			
	% / 1000 Å									
1/9/92	2/9/92	31/10/92	1/11/92							
153 Hilda	3.7 ± 0.2	2.4 ± 0.2	-	3.0 ± 0.9	3.2 ± 0.6	P	P	170	0.062	7.48
153 Hilda	-	3.5 ± 0.2	-	-	-	-	-	-	-	-
334 Chicago	3.4 ± 0.2	3.4 ± 0.2	1.9 ± 0.2	-	2.9 ± 0.9	C	C	156	0.047	7.64
361 Bononia	-	-	-	4.6 ± 0.9	4.6 ± 1.0	P	DP	142	0.045	8.22
958 Asplinda	-	-	8.7 ± 0.2	-	8.7 ± 1.0	D	-	47	0.042	10.71
1212 Francette	5.5 ± 0.2	5.0 ± 0.2	5.6 ± 0.2	3.4 ± 0.9	4.9 ± 1.0	P	P	82	0.040	9.54
1269 Rollandia	10.4 ± 0.2	8.2 ± 0.2	-	11.0 ± 0.9	9.9 ± 1.5	D	D	105	0.047	8.82
1345 Potomac	5.1 ± 0.2	3.4 ± 0.2	-	3.9 ± 0.9	4.1 ± 0.9	P	X	72	0.044	9.73
1439 Vogtia	-	-0.7 ± 0.2	-	1.1 ± 0.9	0.2 ± 1.3	F?	XFU	48	0.051	10.45
1529 Oterma	9.2 ± 0.2	8.5 ± 0.2	8.7 ± 0.2	8.5 ± 0.9	8.7 ± 0.3	D	P:	63	-	10.05
1754 Cunningham	5.0 ± 0.2	5.1 ± 0.2	-	-	5.1 ± 0.1	PD	P	80	0.034	9.77
2246 Bowell	10.2 ± 0.2	10.4 ± 0.2	10.2 ± 0.3	-	10.3 ± 0.1	D	D	44	0.054	10.56
2483 Guinevere	-	-	10.2 ± 0.2	-	10.2 ± 1.0	D	-	44	0.043	10.8
2959 Scholl	-	-	9.9 ± 0.2	-	9.9 ± 1.0	D	-	34	0.050	11.2
3134 Kostinsky	-	-	7.8 ± 0.2	-	7.8 ± 1.0	D	-	50	0.037	10.7
3202 Graff	9.6 ± 0.2	8.8 ± 0.2	-	-	9.2 ± 0.6	D	-	56	-	10.3
3415 Danby	-	-	10.0 ± 0.3	9.7 ± 0.9	9.9 ± 0.2	D	-	32	0.106	10.5
3557 Sokolsky	-	12.0 ± 0.2	-	-	12.0 ± 1.0	D	-	47	-	10.7
3571 Milanstefanik	11.3 ± 0.2	10.8 ± 0.2	-	-	11.0 ± 0.4	D	-	39	0.042	11.1
3577 Putilin	10.2 ± 0.2	8.4 ± 0.2	-	-	9.3 ± 1.3	D	-	44	-	10.8
3694 Sharon	-	-	10.8 ± 0.2	-	10.8 ± 1.0	D	-	45	0.055	10.5
3843 OISCA	-	5.5 ± 0.2	5.4 ± 0.2	3.9 ± 0.9	4.9 ± 0.9	EMP	-	49	-	10.6
3923 Radzievskij	-	-	5.5 ± 0.2	1.6 ± 0.9	3.6 ± 2.8	EMP	-	35	-	11.3
4446 Carolyn	-	11.8 ± 0.2	-	-	11.8 ± 1.0	D	-	39	-	11.1
279 Thule	-	9.9 ± 0.2	-	-	9.9 ± 1.0	D	D	126.6	0.041	8.57

4. Reflectance spectra of Hilda asteroids

The reflectance spectra of the 23 Hilda asteroids observed are presented in Figs. 3–16. All spectra are normalized to unit reflectance at $\lambda = 5500$ Å. More than one spectra appear in all figures, and all except the lowest spectrum in the figures are shifted vertically for clarity. The figures are all to the same scale to facilitate cross-comparison. Where data points exist from the Eight Colour Asteroid Survey (ECAS) by Zellner et al. (1985), these are also plotted in the figures as circles. Due to incomplete removal of the atmospheric bands there are some residuals left in most of the asteroid spectra. The largest residuals are from the atmospheric O_2A band at 7612 Å and the telluric H_2O bands in the red part of the WHT spectra. In some of the spectra from the NTT there are some spurious features short-ward of ~ 4200 Å.

The slopes of the spectra have been determined using the method introduced by Jewitt & Luu (1990), namely a linear least square fit to the spectrum between 4000–7400 Å, with unit flux at $\lambda = 6000$ Å. We have also weighted the least squares fit with the S/N obtained at each wavelength bin of the spectrum. From the obtained spectra we classified the asteroids in the manner described in Paper I. A summary of the resulting slope param-

eters and other relevant data are listed in Table 2. The first four columns list the obtained spectral slopes S' on different nights together with their formal errors. Included in the formal error are the error from the least squares fit, and the error introduced by the solar analogue due to imperfect extinction correction (see Fig. 1). The fifth column shows the adopted mean S' and associated errors of the mean. The true uncertainties in the individual measurements if S' are probably in order of $1\%/10^3$ Å as can be estimated from the scatter in S' for asteroids observed more than once. For this reason, when only one spectrum of an asteroid exists, an absolute error of 1 % in S' is adopted. Also listed in Table 2 is the derived taxonomic class, together with the taxonomic classes obtained by Tholen (1989), when available (i.e. for most asteroids up to number 2246). The last three columns give the diameter and visual albedo from IRAS (Tedesco & Veeder 1992). For asteroids with no IRAS albedo the diameter was calculated using the mean albedo of the Hilda asteroids (0.055), and the absolute magnitudes in the last column are from the Ephemerides of Minor Planets (1996).

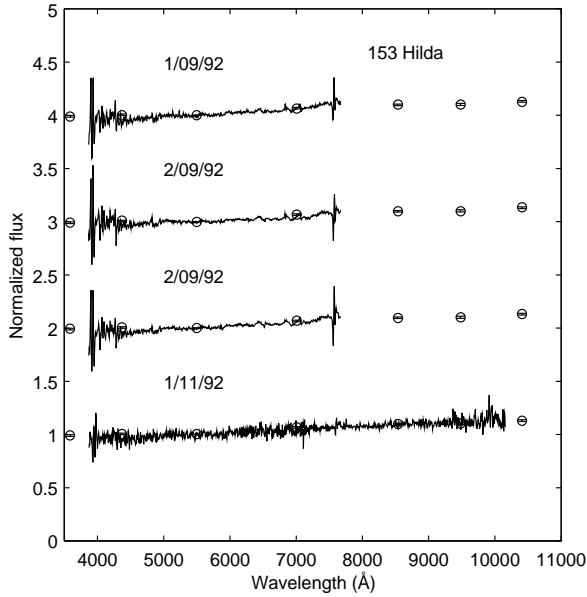


Fig. 3. Reflectance spectra of 153 Hilda.

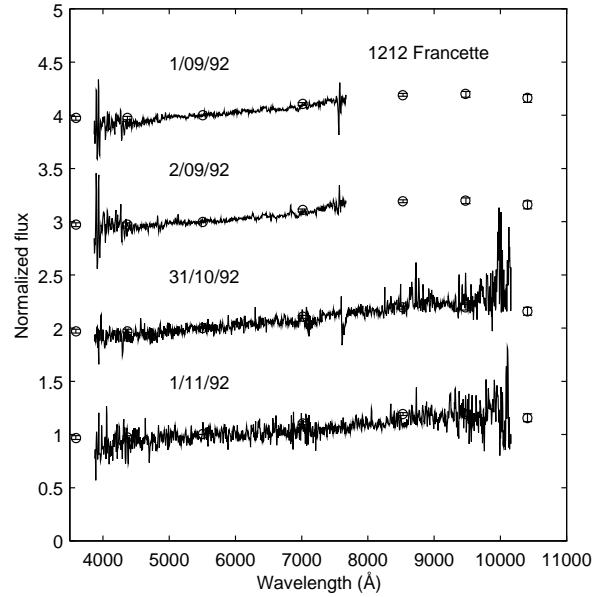


Fig. 5. Reflectance spectra of 1212 Francette.

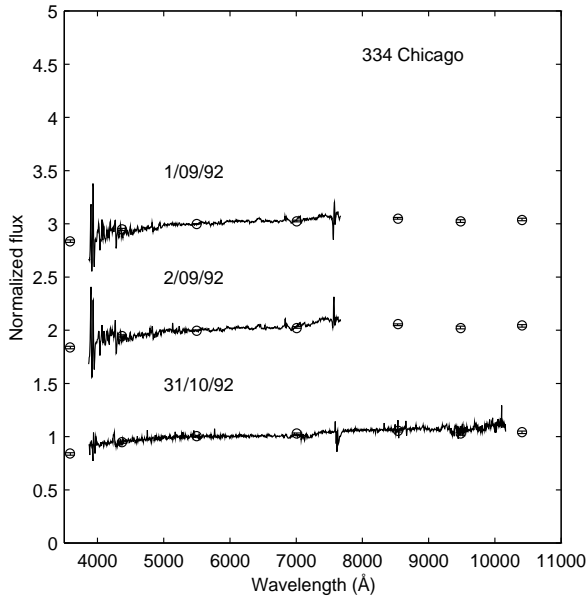


Fig. 4. Reflectance spectra of 334 Chicago.

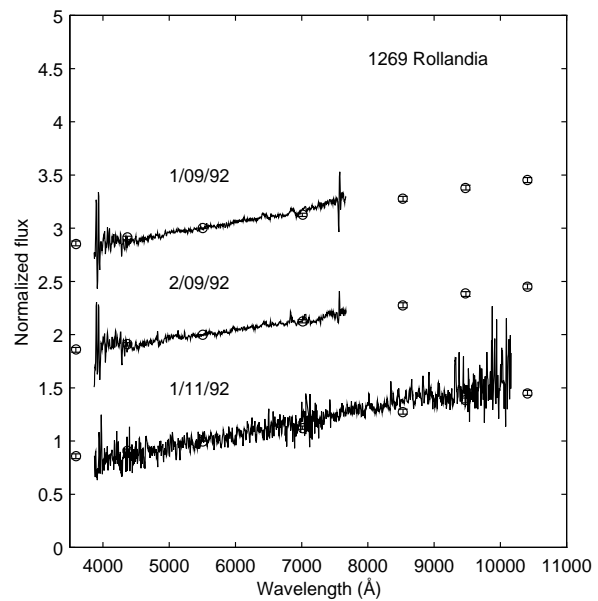


Fig. 6. Reflectance spectra of 1269 Rollandia.

4.1. Absorption features

No evident absorption features are seen in any of the spectra. However, phyllosilicate absorption bands in the visual spectral region only have intensities of a few percent of the continuum and so their apparent absence is not surprising. To be sure that none were present, we made a careful search for absorption bands by fitting polynomials to the spectra, to represent a noiseless ideal spectra of the asteroids. If any absorption bands with greater depth than our detection limit were found in the ideal spectra we take it as a detection of an absorption band. The spectral flux f was fitted to a polynomial p with degrees rang-

ing from 1 to 10. The best fit is the polynomial degree which minimized the sum, Ω

$$\Omega = \sum_{\text{All pixels}} |f - p| \quad (3)$$

The best fitting polynomials were usually of degrees ranging from 8 to 10. Our detection limits are determined from the S/N of the spectra which range between 1–4 % at best and gets worse at the blue and red end of the spectra. Any found absorption bands are described together with the spectra below.

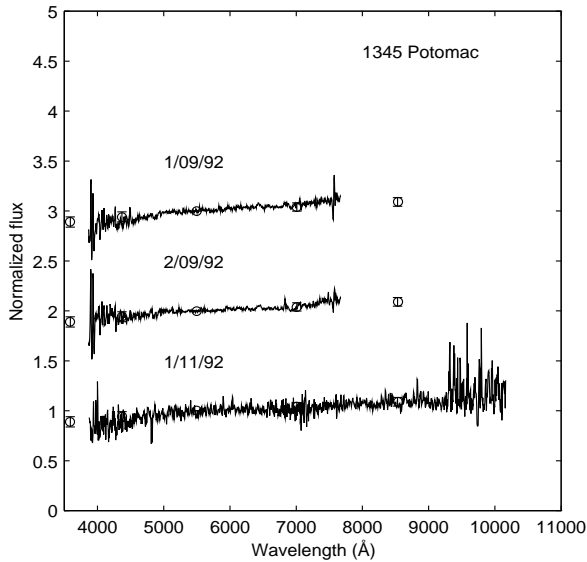


Fig. 7. Reflectance spectra of 1345 Potomac.

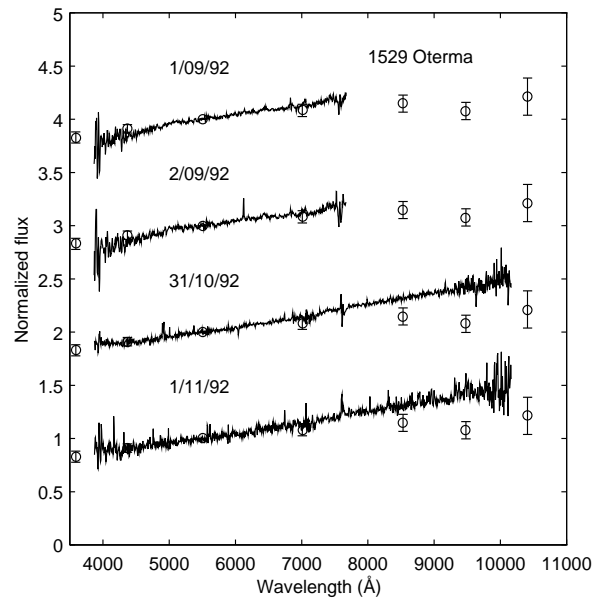


Fig. 9. Reflectance spectra of 1529 Oterma.

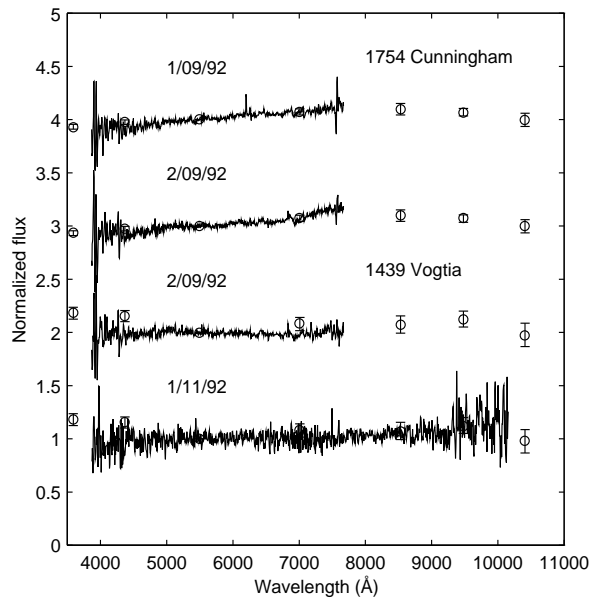


Fig. 8. Reflectance spectra of 1754 Cunningham and 1439 Vogtia.

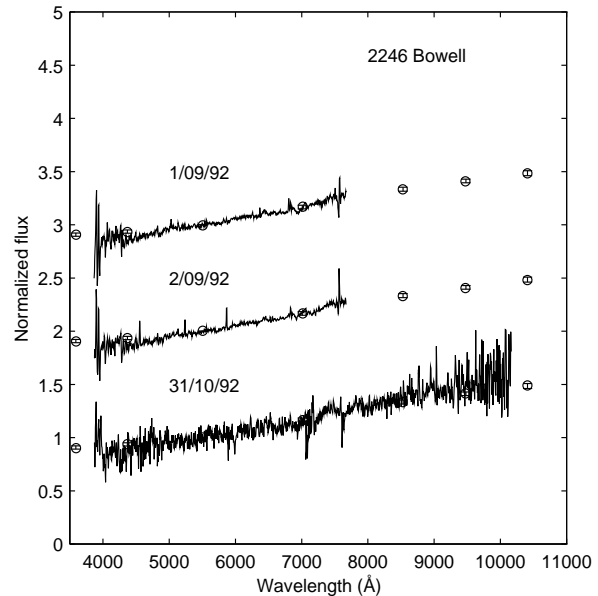


Fig. 10. Reflectance spectra of 2246 Bowell.

4.2. The spectra

153 Hilda. The four spectra obtained of Hilda are shown in Fig. 3. The values obtained for the spectral slope are $S' = 3.7, 2.4, 3.5$ and $3.0 \text{ \%}/10^3 \text{ \AA}$. All, but the $S' = 2.4 \text{ \%}/10^3 \text{ \AA}$ which is marginally low, are within the formal error of the mean. All four are consistent with the asteroid being of taxonomic class P. This is very different from the spectrum of Hilda obtained by Lazzarin et al. (1996), with $S' = 12.3 \text{ \%}/10^3 \text{ \AA}$. Our value is much more consistent with earlier published values. Using the rotation period of 5.11 hours given by Lagerkvist et al. (1996) the relative rotational phases for the three NTT spectra were 0.0, 0.3 and 0.7. The similarity between the three spectra indi-

cates that there is probably no large scale surface variegation on Hilda. The similarity of the WHT spectrum to these three also supports this. However, the time interval between the WHT and the NTT observations is too large to allow a determination of the rotational phase with the known accuracy of the period.

334 Chicago. This is the only asteroid among the Hilda asteroids observed that was found to be of C class. Our spectra (Fig. 4) have spectral slopes of 3.4, 3.4 and $1.9 \text{ \%}/10^3 \text{ \AA}$ and all three values are consistent with both ECAS photometry and the spectra obtained by Vilas & Smith (1985). The obtained tax-

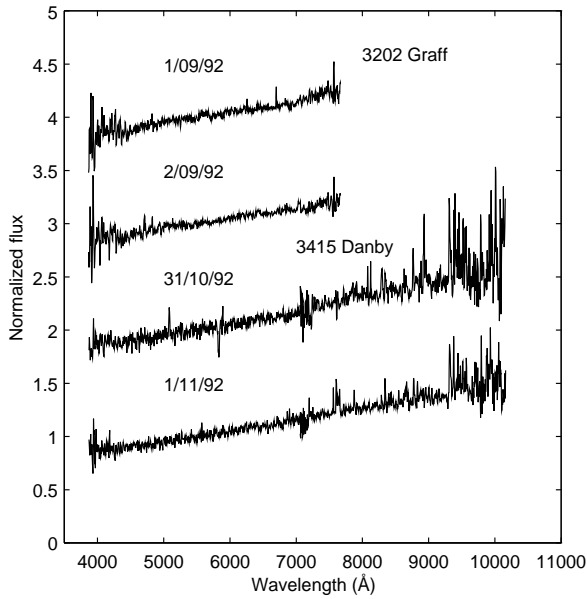


Fig. 11. Reflectance spectra of 3202 Graff and 3415 Danby.

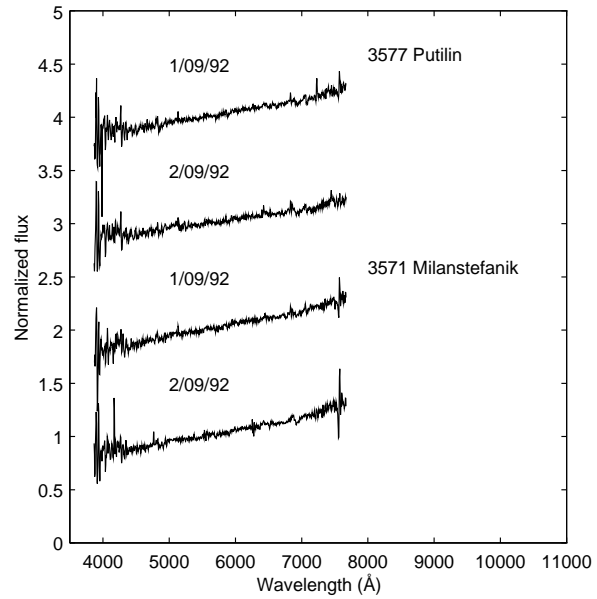


Fig. 12. Reflectance spectra of 3577 Putilin and 3571 Milanstefanik.

onomy (C class) agrees with Tholen (1989). Absorption edges arising from inter-valence charge transfer (IVCT) from the Fe^{2+} cation is seen in the blue part ($\lambda \simeq 5000\text{\AA}$) of the spectra. There is also indication of a broad and very shallow absorption feature centered around 7000\AA , and this is probably due to $\text{Fe}^{2+} - \text{Fe}^{3+}$ charge transfer in phyllosilicates. However, both these features are significantly less intense than those seen in spectra of CM2 carbonaceous chondrites (Vilas et al. 1993c).

361 Bononia. Our spectrum (Fig. 15) is somewhat less red than the ECAS photometry for $\lambda > 7000\text{\AA}$. A spectral slope of $4.6\% / 10^3\text{\AA}$ from our spectrum indicates the taxonomic class as P while Tholen classified Bononia as DP-type. However, our spectral slope is close to the DP, PD range.

958 Asplinda. Our spectrum, shown in Fig. 15, gives a spectral slope of $8.7\% / 10^3\text{\AA}$ indicative of a D-type taxonomy. There is no sign of the large reflectivity drop seen in the ECAS data points at 8530\AA and 9480\AA . The large error bars in the ECAS data associated with these two points make them less reliable.

1212 Francette. Three of our four spectra are consistent with the ECAS photometry and have spectral slopes of 5.5 , 5.0 and $5.6\% / 10^3\text{\AA}$ (Fig. 5). The last spectrum from the WHT has a smaller slope $S' = 3.4\% / 10^3\text{\AA}$, and may indicate a marginal detection of surface variegation. However, all four spectra indicate a P taxonomy in accordance with Tholen (1989). A spectrum was obtained by Vilas & Smith (1985) which is consistent with ours except for the up-turn at the blue end ($0.6\text{-}0.7\mu\text{m}$) of their spectrum.

1269 Rollandia. The three spectra of Rollandia (Fig. 6) show somewhat different spectral slope ($S' = 10.4$, 8.2 and 11.0

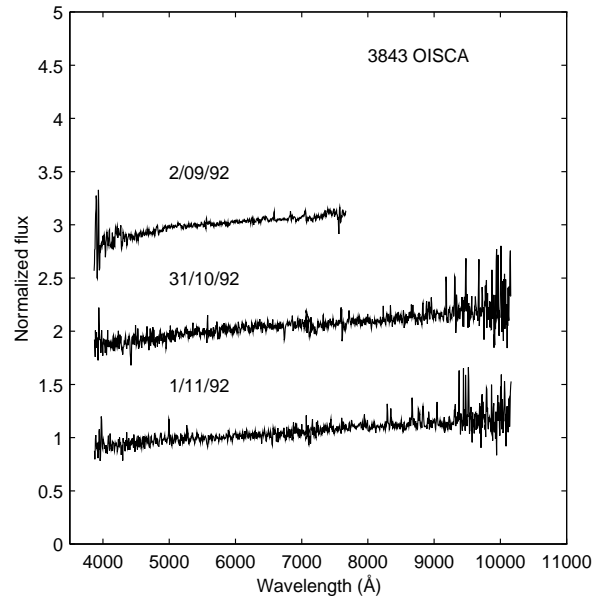


Fig. 13. Reflectance spectra of 3843 OISCA.

$\% / 10^3\text{\AA}$) none being within the formal errors of each other. Again this may be a marginal detection of surface variegation. The September 2 spectrum with $S' = 8.2\% / 10^3\text{\AA}$ is the most consistent with the ECAS photometry. All slopes suggest a D-type, consistent with the classification by Tholen (1989). Vilas & Smith (1985) obtained a spectrum of Rollandia which is consistent with our except for the flattening at the blue end ($0.6\text{-}0.7\mu\text{m}$) of their spectrum.

1345 Potomac. The spectra of Potomac are shown in Fig. 7 have $S' = 5.1$, 3.4 , and $3.9\% / 10^3\text{\AA}$. Two are self-consistent

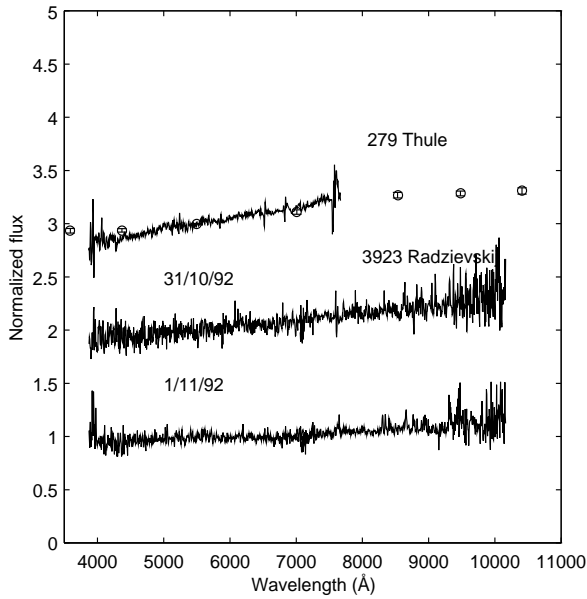


Fig. 14. Reflectance spectra of 279 Thule and 3923 Radzievskij.

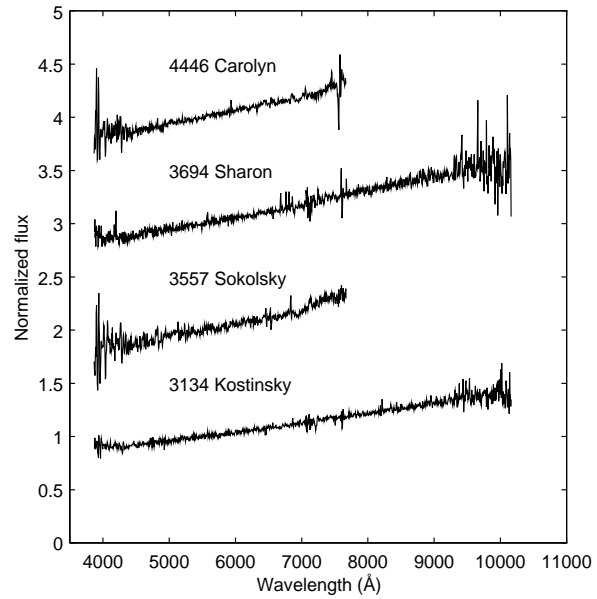


Fig. 16. Reflectance spectra of 4446 Carolyn, 3694 Sharon, 3557 Sokolsky, and 3134 Kostinsky.

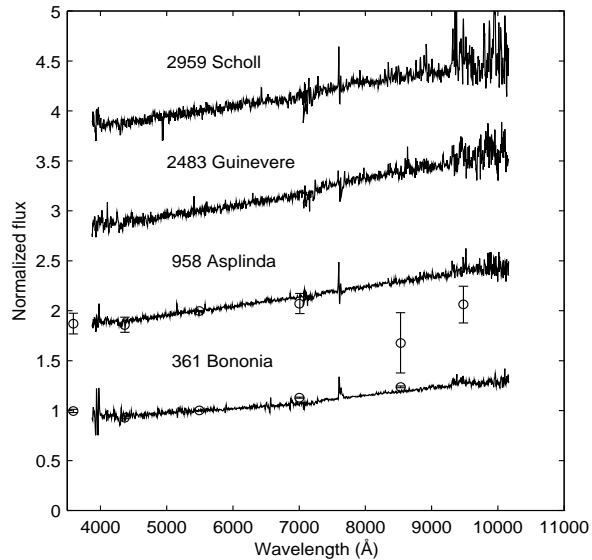


Fig. 15. Reflectance spectra of 2959 Scholl, 2483 Guinevere, 958 Asplinda and 361 Bononia.

with the third being rather high. Photometry from ECAS is in agreement with our spectra. Two of the calculated spectral slopes are indicative of a P taxonomy, that is $S' < 5.0 \text{ \%}/10^3 \text{ \AA}$. One though, is near the limit between the P and PD class. Tholen (1989) classified Potomac as X, but the low IRAS albedo (Tedesco & Veeder 1992) suggests that a P taxonomy is more likely.

1439 Vogtia. The two obtained spectra are shown in Fig. 8. Vogtia's spectrum on September 2 has a slightly negative spectral slope ($S' = -0.7 \text{ \%}/10^3 \text{ \AA}$) and on November 1 the spectrum is slightly reddish, with $S' = 1.1 \text{ \%}/10^3 \text{ \AA}$. The consis-

tency with ECAS photometry on November 1 is good, and it is clear that the spectral slope is very shallow. This asteroid was given the unusual XFU classification by Tholen (1989). The most plausible taxonomic type of Vogtia is F, due to the very flat or even slightly blue spectra and the weakness of any UV absorption bands.

1529 Oterma. The four spectra of Oterma (Fig. 9) all show very similar slopes ($S' = 9.2, 8.5, 8.7$ and $8.5 \text{ \%}/10^3 \text{ \AA}$) and indicate a D-type taxonomy. Tholen (1989) using low quality data classified it as P-type. Compared to ECAS photometry there is a large discrepancy at $\lambda > 7000 \text{ \AA}$, where ECAS show a wide absorption feature centered at the 9480 \AA pass-band. The two WHT spectra does not show this feature while the two NTT spectra end at $\lambda = 7650 \text{ \AA}$. Unpublished photometry made by Dahlgren & Lahulla (private communication) indicate a rotation period ~ 38 hours. The two WHT spectra were obtained about 24 hours apart, i.e. at a relative rotational phase of 0.0 and 0.6. This decreases the possibility that the discrepancy with ECAS and our spectra is due to surface variegation.

1754 Cunningham. Both spectra are very similar (Fig. 8) with $S' = 5.0$ and $5.1 \text{ \%}/10^3 \text{ \AA}$. Cunningham is therefore near the classification border between P and PD types. We classify it as PD-type while Tholen (1989) classified it as P. The ECAS photometry is in agreement with our two spectra. Unfortunately our spectra from the NTT do not reach far enough into the red to verify the decrease in reflectivity seen in the ECAS photometry at $\lambda > 8200 \text{ \AA}$.

2246 Bowell. There is an excellent self-consistency in our three spectra of Bowell (Fig. 10) with $S' = 10.2, 10.4$ and

10.2 %/10³ Å . A D-type taxonomy is evident and is in agreement with Tholen (1989). Bowell was also observed by Vilas & Smith (1985) and their spectrum is consistent with ours except for the flattening at the blue end (0.6-0.7 μm) of their spectrum.

2483 Guinevere. Only one spectrum using the WHT was obtained. This has a spectral slope of 10.2 %/10³ Å and on the basis of this we classify it as a D-type asteroid (Fig. 15).

2959 Scholl. One WHT spectrum was obtained (Fig. 15). This has a spectral slope of 9.9 %/10³ Å , hence Scholl appears to be a typical D-type asteroid.

3134 Kostinsky. The spectral slope $S' = 7.8$ %/10³ Å of the only spectrum obtained using the WHT makes Kostinsky a D-type asteroid (Fig. 16). There is no sign of any absorption bands in the spectrum, even-though it has an extremely high S/N ratio.

3202 Graff. Both NTT spectra indicate a D-type taxonomy (Fig. 11) as the spectral slope is 9.6 and 8.8 %/10³ Å .

3415 Danby. The two WHT spectra show good internal consistency with $S' = 10.0$ and 9.7 %/10³ Å (Fig. 11). The taxonomy from this is clearly a D-type. However, it appears to have an anomalously high albedo (Table 2). This is may be due to Danby's very short rotation period ~ 3 hours (Dahlgren & Lahulla, private communication), and the shortcomings of the method of albedo determination in these cases. This is further discussed in Sect. 5.

3557 Sokolsky. The one spectrum (Fig. 16), obtained with the NTT, has the largest slope of the observed asteroids spectra ($S' = 12.0$ %/10³ Å), indicative of a D-type asteroid.

3571 Milanstefanik. The two NTT spectra show good agreement with each other, having slopes of $S' = 11.2$ and 10.8 %/10³ Å (Fig. 12). These slopes clearly indicate that Milanstefanik is a D-type asteroid.

3577 Putilin. There is some difference in spectral slope between the two nights ($S' = 10.2$ and 8.4 %/10³ Å). However, both spectra obtained with the NTT (Fig. 12) indicate a D-type asteroid.

3694 Sharon. Sharon's reflectance spectra obtained with the WHT is shown in Fig. 16. With a slope of $S' = 10.8$ %/10³ Å , the spectra indicate that Sharon is a D-type asteroid.

3843 OISCA. Two spectra were obtained with the WHT and one with the NTT (Fig. 13). The spectral slopes are $S' = 5.5$, 5.4 and 3.9 %/10³ Å . OISCA is hence classified as EMP due to the unknown albedo.

3923 Radzievskij. The two spectra both obtained with the WHT (Fig. 14) show a pronounced difference in slopes, S' being measured as 5.5 %/10³ Å on October 31 and 1.6 %/10³ Å on November 1. This difference is much larger than for any of the other observed asteroids. Even if there existed unknown systematic errors in our slope determinations (unlikely given the good agreement with ECAS photometry for other asteroids), this large change in S' is not seen in any other asteroid observed at the same time, indicating that this is a real effect. Therefore 3923 Radzievskij offers the best evidence to date of surface variegation in an outer belt asteroid. Both spectral slopes give a EMP taxonomy.

4446 Carolyn. This asteroid was observed once with the NTT (Fig. 16). It is one of the reddest spectra of our observed asteroids with $S' = 11.8$ %/10³ Å , making it clearly a D-type asteroid.

279 Thule. Thule is the only numbered asteroid in the 4:3 resonance with Jupiter at 4.3 AU. Our spectrum shown in Fig. 14 has a $S' = 9.9$ %/10³ Å which is redder than the spectra by Fitzsimmons et al. (1994) and Jewitt & Luu (1990). Compared to ECAS there is also some discrepancy in the blue. However, all spectral slopes are larger than 7 %/10³ Å , for which a D-type classification is assigned.

4.3. Phase reddening

The progressive reddening of asteroid broad-band colours with increasing solar phase angle is an effect that has been known for a long time. Gehrels (1970) found the phase reddening in the B – V and U – B colours of 4 Vesta to be 0.0018 and 0.0027 mag/degree, respectively. Lumme & Bowell (1981) give mean phase reddening for 20 C-type asteroids, corresponding to 0.15 ± 0.12 %/10³ Å /degree in B – V. The spectral slope S' is determined for a wavelength interval corresponding more to a B – R colour, and so the B – V phase reddening gives a lower limit of phase reddening that may be present in S' when C-type material is considered. However, we emphasize that the above is an estimate of the *mean* phase reddening made for C-types, while all except one of our spectra indicate P- and D-type asteroids.

To search for phase reddening effects in our data we have plotted in Fig. 17 the derived values of S' and the solar phase angle for each asteroid classed by us as D-type (top diagram) and P-type (bottom diagram). A linear least squares fit to this data gives a phase reddening of 0.04 ± 0.03 %/10³ Å /degree for D-types and 0.003 ± 0.05 %/10³ Å /degree for P-types. It thus appears that the phase reddening effect is negligible for the taxonomic P and D classes. The S' used in the discussion will therefore not be corrected to zero phase angle.

4.4. Dependence of the taxonomy on asteroid size

Internal comparisons between the Hilda asteroids are less hampered by selection biases than usually is the case for observa-

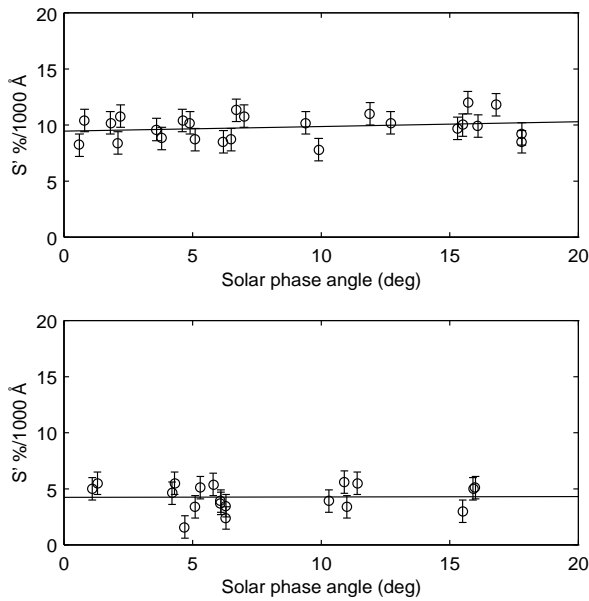


Fig. 17. Spectral slope for D and P-type Hilda asteroids versus phase angle. The linear least squares fit to the data gives a phase reddening of $0.04 \pm 0.03 \text{ \%}/10^3 \text{ \AA}/\text{degree}$ for D-types and $0.003 \pm 0.05 \text{ \%}/10^3 \text{ \AA}/\text{degree}$ for P-types.

tional data for the following reasons; (i) all Hilda asteroids have orbits with very similar semi-major axis, (ii) for Hilda asteroids with known albedo, the P and D-types have very similar albedos, implying that for a given size range the probability of discovering a P-type or a D-type asteroid are similar if numbers are equal. This eliminates a possible bias due to different albedos among the P and D-types in the Hilda group. As we observed all numbered Hilda asteroids at low airmass during the observing nights, we did not introduce any bias by observing only some of the targets available at low airmass. This supports that there is very little observational bias in our sample, at larger sizes than the approximate cut-off size ($D \sim 40 \text{ km}$).

The spectra of 3843 OISCA and 3923 Radzievskij could not be classified uniquely, but in the following discussion they will be assumed to be P-types given their spectral slopes. This is justified by the large heliocentric distance of the Hilda group, making it very probable that they in fact are P-types and not E or M-type asteroids.

It is immediately seen that all Hilda asteroids that were classified for the first time in this investigation, with the exception of the above mentioned, 3843 OISCA and 3923 Radzievskij, are of type D. At the time of writing there are 1 C, 18 P, 22 D and 3 PD or DP asteroids known in the Hilda group, giving percentages of 2% C, 28% P, 34% D and 5% DP or PD's in the group. These percentages are in contrast to those shown in figure 1 of Tedesco & Gradie (1982) which indicate the C, P and D's in the Hilda group as roughly equally divided at 1/3 each. Also, the bias corrected distribution by Gradie et al. (1989) do not agree with our data. Their distribution has roughly 65 %, 20 % and 10 % fractions of P, D and C-types. However, the Tedesco

& Gradie (1982) and Gradie et al. (1989) work was based on a much smaller number of Hilda asteroids with known taxonomy, and consequently, their result was rather uncertain. At the moment there is one C-type (334 Chicago) in the Hilda group, and Tholen (1989) only lists two C-types among the Trojan asteroids. The almost complete absence of C-type asteroids, outside of the Cybele group suggest that the C population is confined at smaller heliocentric distance than earlier believed.

Fig. 18 shows histograms of the size distributions for Hilda asteroids, those classified as P or D-type and the whole group. It is clearly seen that the P-type distribution peaks at a larger diameter than the D-types. More specifically, all but one (334 Chicago of type C) of the asteroids larger than 125 km are P-types while the largest D-type is 105 km. The fraction of D-types in the 75 km size bin is 22 % while in the 50 km bin the fraction of D-types has increased to 48 %. The corresponding numbers for the P-types are 78 % and 13 %, respectively. The 75 km bin is completely sampled, while the 50 km bin is 61 % sampled, but here additional asteroids will in the future be added from the unnumbered population and possibly from new discoveries. This trend with an increasing fraction of D-type asteroids at smaller sizes seems to continue also into the 25 km size bin. However, here the sampled population is too small to draw any firm conclusions. The mean diameter for the P-types is 85 km whereas the mean diameter for the D-types is only 49 km. This difference in mean diameter is statistically significant at $> 99 \text{ \%}$ level. Fig. 19 shows the spectral slope plotted versus asteroid diameter. The large number of D-types at smaller sizes is clearly seen as a cluster of S' values around $10 \text{ \%}/10^3 \text{ \AA}$. The correlation coefficient r of S' with asteroid size D is $r = -0.67$, and a linear least squares fit to the data give $S' = -0.05D + 11.3$, close to the Paper I result ($S' = -0.07D + 11.9$). The statistical significance of $r = -0.67$ with 33 data points is $> 99 \text{ \%}$. This confirms our earlier result in Paper I, in which the spectra of the smaller ($D \sim 50 \text{ km}$) of the observed Hilda asteroids were found to be primarily D-type.

The results presented above and in Figs. 18 and 19 show strong evidence for a correlation between spectral slope/asteroid taxonomy with asteroid size, in such a way that D-type asteroids are significantly more numerous at smaller diameters. The P-types dominate at larger sizes ($D \sim 80 \text{ km}$), implying different size distribution for P and D-types. This is also supported by similar correlation for the Trojan asteroids as suggested by Jewitt & Luu (1990) and the D-types observed by Fitzsimmons et al. (1994). In contrast, however, no such size dependence was seen by Xu et al. (1995) among small main belt asteroids, implying that this effect may only occur for the primitive taxonomic classes.

5. Discussion

There are a number of secondary effects not intrinsic to the surface composition of the asteroid which may distort our result, especially if these secondary effects have a large heterogeneity among the asteroids in the Hilda group. Examples of these secondary effects are mean particle size of the regolith, surface

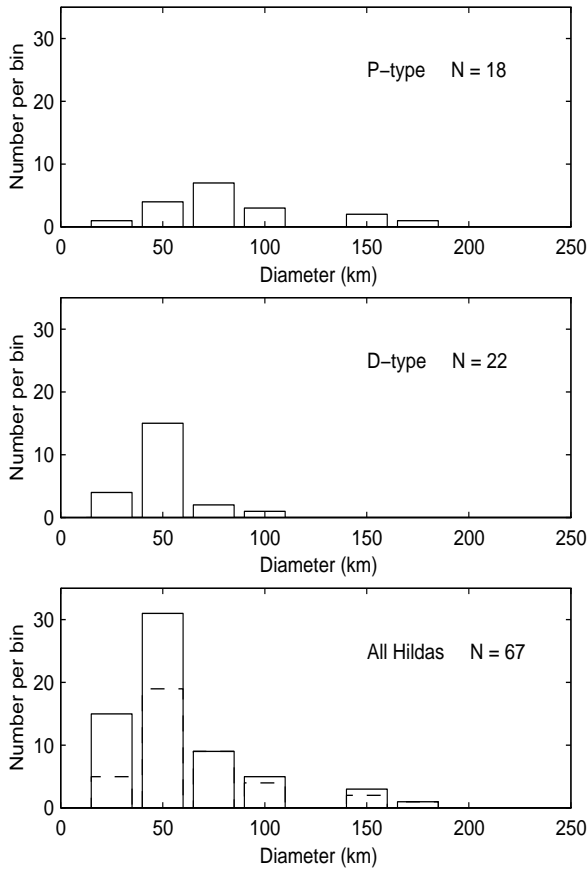


Fig. 18. The size distribution for Hilda asteroids classified as P or D-type and all numbered Hilda asteroids. The dashed lines indicates the number of classified asteroids as P or D-type in each bin. Note that the 175 and 75 km bins are fully sampled. Used bin size is 25 km.

temperature, viewing geometry and effects of shocks induced by collisions. Below we will argue that some of the secondary effects are negligible, while others are very difficult to constrain.

The colour of minerals are known to vary with viewing geometry (Gradie et al. 1980). However, the variation only becomes significant at large phase angles, while the colour variations decrease with increasing albedo. In our case, the absence of an observed phase reddening effect discussed in Sect. 4.3 strongly suggests that this was a minor effect. The asteroids were all observed close to opposition ($\alpha < 18^\circ$) giving similar viewing geometry for all objects which will also minimize the effect.

The size of the regolith particles is of importance. Clark et al. (1992) showed that the existence of smaller particles and of recrystallized material after melting both increases the spectral slope. They used chondritic material for their experiment which is not realistic for P and D-type asteroids, but nevertheless, their result may be relevant to P and D-type material. Unfortunately, we do not have any constraints on the particle size of the regolith, and also the possible chock and melting events caused by collisions are very difficult to constrain in detail. However, what can be said is that it is difficult to imagine collisional processes

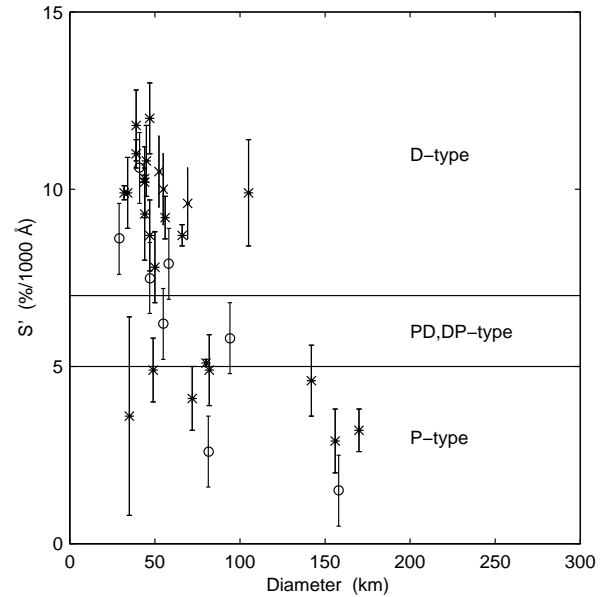


Fig. 19. Spectral slope as a function of asteroid diameter. The '*' indicate our data, the 'x' are data from Fitzsimmons et al. (1994) and 'o' are from Paper I. Horizontal lines indicate the S' -zones corresponding to different taxonomies. To increase the clarity of the figure the error in the IRAS diameters are not shown; their formal errors are usually less than 5 km.

that preferably make small particles accumulate on the surface. Laboratory experiments by Nakamura & Fujiwara (1991) also suggests larger ejection velocities for smaller fragments, which would lead to a preferential loss from the asteroid of small particles rather than a gain.

If the surface temperature varies over the sun-lit hemisphere of the asteroid this may affect the shape and position of absorption bands (Singer & Roush 1985). As we do not see any absorption bands and the classification was made on the basis of the spectral slope, the temperature probably has a minor effect on our spectra. A possibly more important contribution from the surface temperature, together with the objects rotational period and pole orientation, comes through the used radiometric method to determine asteroid diameters and albedos (Spencer et al. 1989). They show that the Standard Thermal Model (STM) used to model the IRAS fluxes will underestimate the diameter and overestimate the albedo for cool, rapidly rotating asteroids. This may influence the spectral slope - asteroid size relation found. The determined diameter for a few Hilda asteroids may be seriously ($\sim 30\%$) underestimated due to their rapid rotation (3415 Danby is one possible candidate, Dahlgren & Lahulla, private communication). This effect may place more D-type asteroids in the 'large' category, but does not explain the absence of other types in the 'small' categories.

5.1. Possible origin of the spectral slope - size relation

The scenario outlined by Bell et al. (1989) suggests a condensation sequence starting with D-types as the most primitive ob-

jects, running through the P class and on to the C class, which then are the most altered among these types of objects. There are supporting evidence for this scenario in the correlation of the C-P-D classes with heliocentric distance, and thus, probably with decreasing thermal metamorphism, which may be the dominant cause of this taxonomy sequence. Further support comes from the presence of phyllosilicate absorption bands in many C class asteroids in the 2.8-3.5 AU zone of the asteroid belt, but only in a few P-types (Vilas & Gaffey 1989). This point is further supported by our spectra, as no phyllosilicate absorption features were found in any of the P or D-type asteroids observed. This strongly suggest that aqueous alteration could principally not take place at a heliocentric distance of 4 AU due to too low temperatures and that the P and D-types are generally anhydrous. Further support is found from the $3\mu\text{m}$ work done by Jones et al. (1990). Assuming that the main cause for the different composition of C, P and D-types are due to varying degree of thermal evolution, (which is suggested by the above), there is a need for a size-dependent heating mechanism to explain the spectral slope - size relation found among the Hilda asteroids. This mechanism is also required to increase the amount of heating for larger bodies. This is somewhat troublesome, as the P and D-types seem to be anhydrous, requiring the heating mechanism to be weak enough not to melt a significant amount of the ice, that is believed to be incorporated in the asteroids, but able to change the spectral properties of the surface.

The mechanisms usually discussed in the context of heating asteroids are heating by short-lived radio-active species (e.g. ^{26}Al) and Electrical Induction Heating (Lebofsky et al. 1989, and references therein). There are several reasons why severe heating by ^{26}Al may be questionable, even though it favors the heating of large objects which may be the cause of the spectral slope - size relation. The main two objections are; its insensitivity of the asteroids position in the asteroid belt, which is contradicted by the distribution of the taxonomic types indicating much more heating in the inner parts of the asteroid belt (Bell et al. 1989; Gradie et al. 1989), and second, the two largest asteroids, Ceres and Pallas, which should have been most heated by ^{26}Al , show no evidence of this. The low inferred amount of ^{26}Al in meteorites are usually also quoted as an argument against ^{26}Al . However, in our case, we want a heat source that mildly can heat the larger asteroids.

Electrical induction heating was proposed by Sonett et al. (1968) as a possible heat source due to the intense solar wind during the Sun's T-Tauri stage, inducing electrical currents through the asteroid. Since there are a number of factors involved in this process, both including bulk material properties as the electrical conductivity, and the intensity and duration of the plasma out-flow, it is difficult to determine the total heat input to an asteroid. However, models by Herbet (1989) show that heating peaks at a certain size, and declines for both increasing and decreasing sizes around this peak. The maximum temperature are usually obtained for objects between 20 - 100 km in size. Electrical induction heating may then explain the seemingly diverse heating history of individual asteroids at a similar distance from the Sun. However, the spectral slope - size correlation indicates

less heating at $D \sim 50$ km which is not favored by the electrical induction process.

An alternative scenario can be put forward, assuming that the intensity of the heating episodes discussed above was similar for all objects in the Hilda zone and rendered similar compositions for the objects. This was followed by a subsequent size-dependent evolution of the asteroids surface composition causing the observed spectral slope - size relation. The main size-dependent physical process acting on the asteroids are their mutual collisions, reshaping the original properties of the objects in the belt. For instance, if D-types are more fragile than P-types, this will favor disruptive collisions among D-type precursors. In this case, a larger fraction of the smaller body population can be collisional fragments from a few shattered large D-type precursors, thereby resulting in a large fraction of small D-type asteroids as observed. Also, the smaller the asteroids are, the higher is the probability that they are collisional fragments. This implies that the surfaces of larger asteroids on the average are older. They will therefore be preferentially exposed to "space weathering" processes that may effect the optical properties of the surface with time. The space weathering process have been discussed extensively in connection to S-type asteroids (Burbine et al. 1996) and in this case the space weathering depresses absorption features and reddens the spectral slope of the S-type surface materials. If the space weathering has the same effect of P and D-type material this will produce an effect in the opposite direction compared to the spectral slope - size relation with time. Of course will the older surfaces be more heavily cratered, and the heat input from cratering events may change the properties of the surface with time in a way that is consistent with our observations (Clark et al. 1992).

The above discussion points to another possible scenario by combining of the two main points so far trying to explain the size dependent taxonomy - heating and collisional evolution. First, interiors of the objects in the Hilda zone were mildly heated in the early Solar System. Then subsequent collisional evolution stripped some of the larger asteroids, forming preferably P-types from the exposed heated interiors, and preferentially expelling smaller fragments from the less heated upper layers, that today make up the smaller body D-type population. This is one possible scenario that can result in the observed size dependent taxonomy for these primitive groups. That some large asteroids may be the heated interiors of once larger precursors was also put forward by Hiroi et al. (1996) from their study of C, G, B and F-type asteroids.

6. Conclusions

We have presented spectra of 23 Hilda asteroids obtained in 1992. No absorption features were observed in any P or D-type spectra, indicating an anhydrous surface composition. One asteroid, 3923 Radzievskij, was found to have significantly different spectral slopes at two observational epochs. We conclude that this asteroid may possess large surface variegation, possibly due to the existence of a large impact structure on its surface similar to that of 4 Vesta (Drummond et al. 1988).

Surprisingly, we find that the population is dominated by D-type objects, with few P-type and C-type asteroids observed. This finding implies that C-type asteroids are prevalent over a much smaller range of heliocentric distance than originally believed, and that the proportion of P-type asteroids existing in this region of the asteroid belt has also been overestimated.

A strong correlation of spectral slope with size exists for primitive asteroids, confirming earlier finding by both the present authors and other investigators. Importantly, we have shown that this correlation is present in a dynamically distinct population with a very small spread in orbital semi-major axis. The origin of this could either be a size dependent heating effect in the early history of the Solar System, followed by collisional evolution or only due to collisional evolution of the Hilda asteroids. Further investigation of this correlation by observations of smaller bodies may reveal important clues as to which of these processes produced this effect.

Acknowledgements. The William Herschel Telescope is operated on the island of La Palma by the Royal Greenwich Observatory in the Spanish Observatorio del Roque de los Muchachos of the Instituto de Astrofísica de Canarias. J. Lagerros is thanked for discussion on the Standard Thermal Model for asteroids.

References

- Cayrel de Strobel G., 1990, Solar analogs seen at high spectral resolution and very high S/N ratios. In: Sanches F., Vezquez M. (eds.) *New windows to the Universe*. Cambridge Univ. Press, Cambridge, p. 195
- Bell J.F., Davis D.R., Hartmann W.K. et al. 1989, Asteroids: The big picture. In: Binzel R.P., Gehrels T., Matthews, M.S. (eds.) *Asteroid II*, Univ. of Arizona Press, Tuscon. p. 921
- Burbine T. H., Meibom A., Binzel R. P., 1996, *Meteoritics & Planetary Science* 31, 607
- Clark B.E., Fanale F.P., Salisbury J.W., 1992, *Icarus* 97, 288
- Dahlgren M., Lagerkvist C.-I., 1995, *A & A* 302, 907 (Paper I)
- Drummond J., Eckart A., Hege E.K., 1988, *Icarus* 73, 1
- Ephemerides of Minor Planets (1996)* Institute for Theoretical Astronomy, St. Petersburg.
- Fitzsimmons A., Dahlgren M., Lagerkvist C.-I., Magnusson P., Williams I.P., 1994, *A & A* 282, 634
- Gaffey M.J., Bell J.F., Cruikshank D.P., 1989, Reflectance spectroscopy and asteroid surface mineralogy. In: Binzel R.P., Gehrels T., Matthews, M.S. (eds.) *Asteroid II*, Univ. of Arizona Press, Tuscon. p. 98
- Gehrels, T., 1970, Photometry of asteroids. In: Dollfus, A. (ed.) *Surfaces and interiors of planets and satellites*, Academic Press, p. 319
- Gradie J., Veverka J., 1980, *Nature* 283, 840
- Gradie J., Veverka J., Buratti, B., 1980, *Proc. Lunar Planet. Sci. Conf.* 8th, p. 799.
- Gradie J., Chapman C.R., Tedesco E.F., 1989, Distribution of taxonomic classes and the compositional structure of the asteroid belt. In: Binzel R.P., Gehrels T., Matthews, M.S. (eds.) *Asteroid II*, Univ. of Arizona Press, Tuscon. p. 316
- Herbet F., *Icarus* 78, 402
- Jewitt D. C., Luu J.X., 1990, *AJ* 100, 933
- Jones T. D., Lebofsky L. A., Lewis J. S., Marley M. S., 1990, *Icarus* 88, 172
- King, D.L., 1985, RGO /La Palma Tech. Note No. 31
- Lagerkvist C.-I., Fitzsimmons A., Magnusson P., Williams I.P., 1993, *MNRAS* 260, 679
- Lagerkvist C.-I., Di Martino M., Blanco C., Dahlgren M., Erikson A., Lahulla J.F., Lazzarin M., Lumme K., Pohjolainen S., Riccioli D., 1996, *Earth, Moon and Planets*, 71, 189
- Lazzarin M., Barbieri C., Barucci M.A., 1996, *Astron. J.* 110, 3058
- Lebofsky L.A., Jones T.D., Herbert F., 1989, Asteroid volatile inventories. In: Atreya S.K., Pollack J.B., Matthews M.S., (eds.) *Origin and evolution of planetary and satellite atmospheres*, Univ. of Arizona Press, Tuscon. p. 192
- Lumme K., Bowell E., 1981, *Astron. J.* 86, 1705
- Luu J., Jewitt D.C., Cloutis E., 1994, *Icarus* 109, 133
- Nakamura A, Fujiwara A., 1991, *Icarus* 92, 132
- Singer R.B., Roush T.L., 1985, *J. Geophys. Res.* 90, 12434
- Sonett C.P., Colburn D. S., Schwartz K., 1968, *Nature* 219, 924
- Spencer J.R., Lebofsky L.A., Sykes M.V., 1989, *Icarus* 78, 337
- Tedesco E.F, Gradie J., 1982, *Science* 216, 1405.
- Tedesco E.F, Veeder G.J., 1992a, IMPS albedo and diameters catalog. In: Tedesco, E.F., (eds.) *Infrared Astronomical Satellite Minor Planet Survey*. Phillips Laboratory Technical Report No. PL-TR-92-2049. Hanscom Air Force Base, MA. p. 243
- Tholen D.J, Barucci, M.A., 1989, Asteroid taxonomy. In: Binzel R.P., Gehrels T., Matthews, M.S. (eds.) *Asteroid II*, Univ. of Arizona Press, Tuscon. p. 298
- Tüg H., 1977, *Messenger* 11, p. 7
- Vilas F., Smith B.A., 1985, *Icarus* 64,503
- Vilas F., Gaffey M.J., 1989, *Sci* 246, 790
- Vilas F., MacFadden, L. A., 1992, *Icarus* 100, 85
- Vilas F., Hatch E.C., Larson S.M., Sawyer, S.R., Gaffey, M.J., 1993a, *Icarus* 102, 225
- Vilas F., Larson S.M., Hatch E.C., Jarvis K.S., 1993b, *Icarus* 105, 67
- Vilas F., Hiroi T., Zolensky M. E., 1993c, *Proc. Lunar Planet. Sci. Conf.* 24th, p. 1465
- Vilas F., Jarvis K.S., Gaffey M.J., 1994, *Icarus* 109, 274
- Xu S., Binzel R.P., Burbine T.H., Bus S.J., 1995, *Icarus* 115, 1
- Zellner B., Tholen D.J., Tedesco E.F., 1985, *Icarus* 61, 355